

NUMERICAL APPROACH TO SIMULATE THE MECHANICAL BEHAVIOUR OF METAL SEALS IN LID SYSTEMS OF DUAL PURPOSE CASKS UNDER STORAGE CONDITIONS

Linan Qiao¹, Sven Nagelschmidt¹, Uwe Herbrich¹,
Uwe Zencker², Dietmar Wolff², Holger Völzke³ and Ulrich Probst⁴

¹ Researcher, Bundesanstalt für Materialforschung und -prüfung, Berlin, Germany

² Head of working group, Bundesanstalt für Materialforschung und -prüfung, Berlin, Germany

³ Head of division, Bundesanstalt für Materialforschung und -prüfung, Berlin, Germany

⁴ Technical Senior Civil Servant, Bundesanstalt für Materialforschung und -prüfung, Berlin, Germany

ABSTRACT

BAM intended to investigate the long-term behaviour of metal seals using a thermal-mechanical coupled finite element (FE) model. Such a kind of model shall describe assembling and assembled state of metal seals in dual purpose casks for dry interim storage of radioactive materials. For the development of those simulation models, an analytical model for the metal seals of type HELICOFLEX[®] HN200 is introduced. For this purpose, a prior developed model with clear physical background is used to describe the decrease of the seal force under the influence of time and temperature under storage conditions. This model was adapted and implemented in the FE program ABAQUS. All parameters of this model are adjusted by test results gathered under laboratory conditions.

INTRODUCTION

The sealing principle of an O-form metal seal used in the lid system of a transport and storage cask is shown in Figure 1. The investigated type of metal seal consists of a close-wound helical spring made of Nimonic[®] steel, a steel inner liner and a ductile pure aluminium (Al-seal) or silver (Ag-seal) outer jacket. During compression, the whole seal is deformed with elastic-plastic deformation. Under the effect of pressure force of the lid system, the combined elastic and plastic deformation provide a very tight contact area between flange and seal outer surface which ensures the leak-tightness of lid systems.

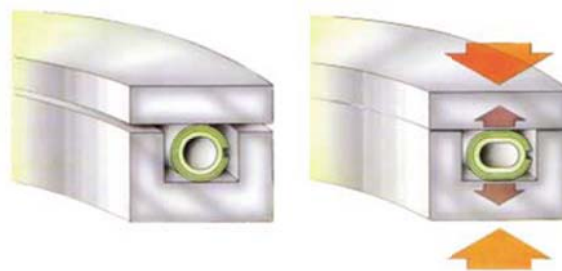


Figure 1. Sealing principle of an O-form metal seal, Garlock (2001).

There are different ways to model metal seals with finite element analyses, see Zencker, et al. (2015), Sassoulas, H. et al. (2006), Shirai, K., et al. (2013) and Ledrappier, F., et al. (2016). One is with a detailed three dimensional (3D) or two dimensional (2D) FE model for each component of seal, another one is with a global ‘gasket element’ model. To study the behaviour of metal seals in detail, for example, the function of each component with different temperatures, friction, elastic and plastic deformation, damage,

material creep behaviour with long time, an appropriate detailed 3D FE model shall be necessary. Contrary to a detailed 3D FE model of those seals, it is more suitable to use a ‘global gasket element model’ to study the performance of metal seals in an entire cask FE model under the influence of environment conditions such as temperature conditions from the decay heat and surroundings as well as mechanical influences such as from accident conditions. Whereat, a ‘global gasket element model’ considers all three components of metal gaskets as one object. Because of simplifications of global gasket element models local strain and stress states in those metal seals cannot be analysed, but rather global values at contact areas between gasket model and cask as well as lid or flange can be determined. All measured data, for example, load/unload-deformation, thermal effect, creep, dynamic reaction, damping, damage, contact area, shear effect, can be used to define a global gasket element model without consideration of “why it is so”. In this work, we consider the global gasket element model and its application in the analysis of a transport and storage cask for radioactive material under interim storage conditions.

Figure 2 a) shows measured data of seal force-compression performances of different specimens, with specific seal force $Y = F / (\pi \cdot d_s)$, F the pressure force of lid system and d_s the overall diameter of a metal seal. Each seal characteristic curve is somewhat different due to design and manufacture tolerances, see different colours in Figure 2 a). The marked points in Figure 2 a) illustrate seal specific conditions, whereat point 2 represents the working point with $\{e_2, Y_2\}$.

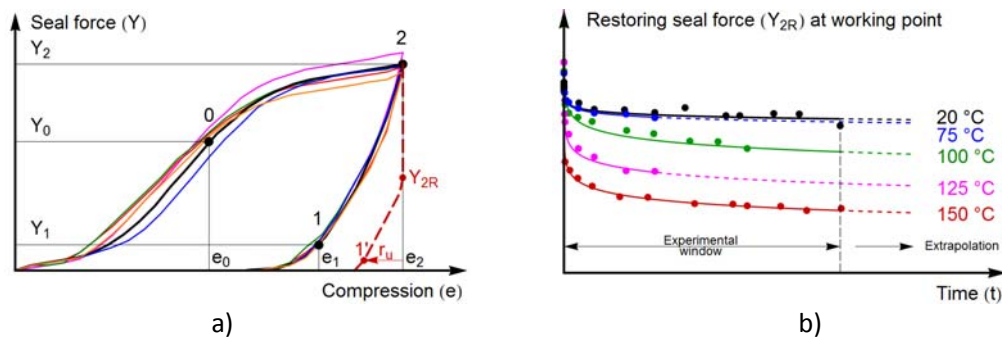


Figure 2. schematically presentation of a) measured seal force-compression curves of an O-form metal seal with different specimens and b) restoring seal forces over time for different temperatures under constant compression conditions.

The seal force decreases during time and with increasing temperature on a lower level to Y_{2R} under constant deformation of e_2 . Also, the remaining elastic displacement r_u decreases, see Figure 2 a) dashed line. The time and temperature dependent decline of Y_2 to Y_{2R} for different test temperatures at selected points in time is diagrammed in Figure 2 b). With higher temperature, the decreasing of seal force with time is accelerated. All of those effects must be considered for the modelling of metal seals.

CALIBRATION OF SEAL BEHAVIOR WITH STATIC LOAD

The characteristic force-deformation curves of seals under investigation are used to calibrate the specific gasket element. For the FE simulation, the program ABAQUS was used. ABAQUS offers different special gasket elements to model sealing behaviour between two components, see ABAQUS (2014). For the calibration of a gasket element under static load without the influence of time, the definition was divided into two parts: load curve and unload (reload) curve. The measured ‘standardised’ load/unload curve, see for example black coloured curve in Figure 2 a), was used to define the static behaviour. Shear

behaviour in radial direction was ignored and the influence of temperature was even not considered. The FE calculation with this load was performed quasi-static with displacement controlled load history.

The cross sections of the modelled HELICOFLEX[®] type of metal seals are shown in Figures 3 a) and 3 b). The helical spring is made of a special nickel alloy (Nimonic[®] 90) with wire diameter of 1.1 mm or 1.2 mm depending on the outer liner material. The inner liner made of stainless steel has a thickness of 0.3 mm for Al-seals or 0.5 mm for Ag-seals. The outer jacket made of aluminium is 0.5 mm thick or 0.3 mm for silver outer jackets. As discussed above, force-compression curves of individual metal seal differ to some extent. As mentioned above, to define the force-compression behaviour, a mean force-compression curve must be derived with statistically confirmed characteristic working point $\{e_2, Y_2\}$, see Figure 2 a) and Figure 4.

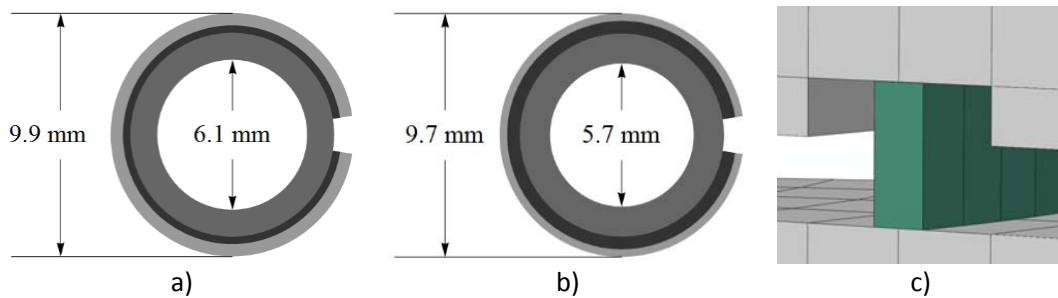


Figure 3. Cross sections of the HELICOFLEX[®] type of metal gaskets according to Garlock (2001) with a) aluminium or b) silver outer jacket and c) corresponding global gasket element.

The investigated seal type was defined as an axial symmetric block with a height in thickness direction equal to the outer diameter and the cross section was simplified to a rectangle, see Figure 3 c). Typical static load/unload/reload curves for investigated Al- and Ag-seals are represented in Figure 4, see Völzke, H., et al. (2013), Probst, U., et al. (2014) and Nagelschmidt, S., et al. (2014).

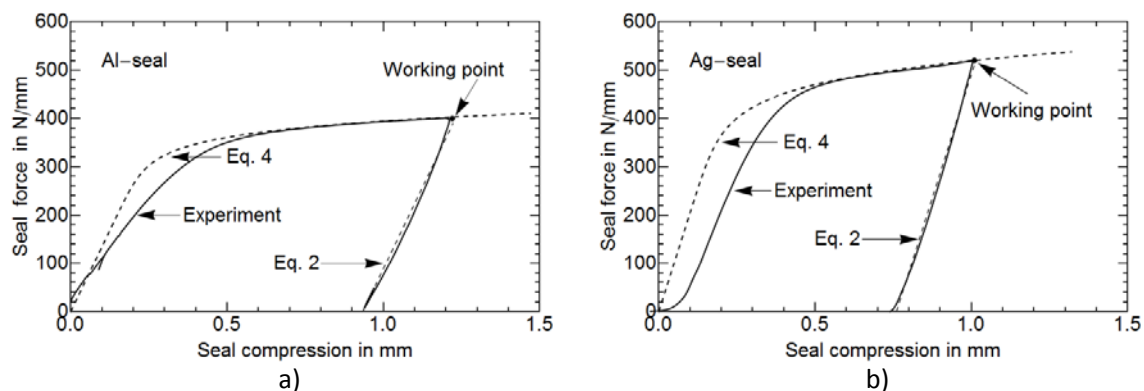


Figure 4. Static force-compression curves of a) Al-seal and b) Ag-seal.

The above described gasket element model is adjusted using the determined static load/unload/reload curves. Therefore, the seal compression e is additive composed into an elastic compression e_e and a plastic compression e_p in the form

$$e = e_e + e_p \quad (1)$$

where the elastic compression can be written as

$$e_e = \frac{Y}{C_0} \quad (2)$$

with seal force Y and elastic stiffness C_0 of observed metal seals. The values of C_0 are determined from unload/reload curves, see Figure 4 and Table 1. The power-law approach in the form

$$e_p = \left(\frac{Y}{C_1} \right)^{C_2} \quad (3)$$

is used for the plastic part of compression in the calculation model. Thus, Equation 1 can be rewritten with Equations 2 and 3 for the (initial) elastic-plastic seal force compression curve in the form

$$e = \frac{Y}{C_0} + \left(\frac{Y}{C_1} \right)^{C_2} . \quad (4)$$

The values of C_1 and C_2 are parameters adjusted to initial load curves in the range from fifty percent seal compression to the working point, see Figure 4 and Table 1. Unload and reload until the elastic range is described by Equation 2 and compression above the elastic range is described by Equation 4, see Figures 4 a) for Al-seals and 4 b) for Ag-seals.

Table 1: used parameters for the static seal model

Seal type	Al-seal	Ag-seal
C_0 in N/mm ²	1350	2050
C_1 in N/mm ²	405	535
C_2	12.5	10.0

Differences between the used model from Equation 4 and measurements in the range from origin to 0.5 mm compression are negligibly especially because of manufacture tolerances among metal seals and their irresistible plastic load behaviour after the first compression (assembling). Whereas, a good adjustment of the calculation model in the region above 0.5 mm for load processes as well as for elastic unload/reload process is essentially.

CALIBRATION OF TIME AND TEMPERATURE DEPENDENT SEAL BEHAVIOUR

In the following, the time and temperature dependent seal behaviour is briefly discussed under assembling conditions with constant deformation of metal seal in a flange system. Under those conditions, BAM investigates metal seals of the abovementioned type with five different constant temperatures in specific developed flange system, see Völzke, H., et al. (2013), Probst, U., et al. (2014) and Nagelschmidt, S., et al. (2014). Results of these investigations are shown in Figure 5. As can be seen, there is a change of the restoring seal force Y_{2R} with time and under the influence of temperature. Because contact surfaces

maintain a constant distance, the decrease of Y_{2R} is equal to a relaxation effect for the global gasket element model. But, with a view to local effects of the three seal components, this decrease is conditioned by thermo-viscoplastic deformation of the ductile outer jacket made of aluminium or silver, which is related to the restored elastic strain energy of the helical spring.

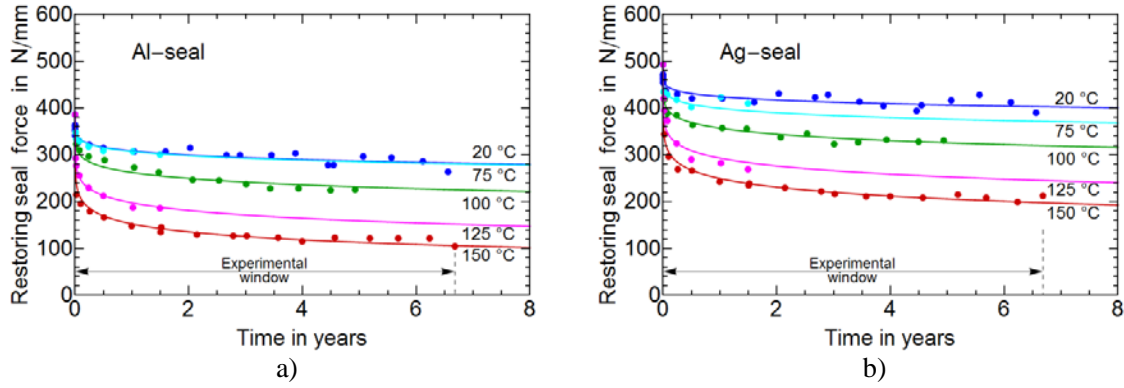


Figure 5. Restoring seal forces of metal seals from type HELICOFLEX[®] with a) Al-seal and b) Ag-seal for five different constant test temperatures.

To describe the decrease of the restoring seal force, BAM developed a calculation model using the time-temperature-superposition (TTS) principle as described in following equation, see the work of Qiao, L., et al. (2016):

$$\bar{Y}_{2R} / Y_2 = \text{Exp} \left[\ln(\bar{Y}_{ref,E} / Y_2) (\alpha_s(\zeta) \tau)^{-\bar{m}} \right] \quad (5)$$

In Equation 5, \bar{m} is a mean value for all of the five different constant test temperatures. The normalised time τ is defined with $\tau = t / t_{ref}$, where t_{ref} is the reference time, defined as 1 year. The time-temperature shift factor is termed as $\alpha_s(\zeta)$ which will be described in Equation 6. Equation 5 satisfies the conditions $\bar{Y}_{2R}|_{\tau=0} = Y_2$ as well as $\bar{Y}_{2R}|_{\tau \rightarrow \infty} = 0$. The latter is conservative due to the fact that seal force values will be never small as zero during operating time. Based on this, the used parameters for investigated seals are given in the following table, Table 2.

Table 2: determined parameters of the mean enhanced power-law model

Seal type	Al-seal	Ag-seal
\bar{m}	0.826	0.846
Y_2 in N/mm	386.0	494.0
$\bar{Y}_{ref,E}$ in N/mm	308.2	424.1

With the application of the TTS principle different shift factors were calculated due to different test temperatures. The relationship between the shift factor as well as the normalized reciprocal absolute temperature can be described with a modified Arrhenius equation, see Nakamura, K., Takayanagi, T. and Sato S. (1989) and Qiao, L., et al. (2017), in the form:

$$\alpha_s(\zeta) = \text{Exp}[B((1 + \zeta_c^{-n})^{-1/n} - (\zeta^{-n} + \zeta_c^{-n})^{-1/n})] \quad (6)$$

Where $\zeta = T_{ref} / T$ is the normalized reciprocal absolute temperature. The reference absolute temperature is defined as $T_{ref} = (20^\circ\text{C} + 273.15)$ in Kelvin. Parameters B , n and ζ_c for Al-seals and Ag-seals are given in the next table, Table 3.

Table 3: determined parameters for the calculation of $\alpha_s(\zeta)$

Seal type	Al-seal	Ag-seal
B	54	52
n	70	57
ζ_c	0.848	0.885

Subsequently, Equations 5 and 6 can be used to estimate the restoring seal force behaviour during time for arbitrary temperatures in the given test temperature range (20 °C to 150 °C). Furthermore, this calculation model was applied to the defined gasket-element. For the consideration of constant or changed seal temperatures, an appropriate function of the determined gasket behaviour from Equations 5 and 6 was implemented in ABAQUS for the gasket element as a function of time and temperature.

SIMULATION OF A LID SYSTEM WITH SEAL FROM ASSEMBLY TO STEADY-STATE AS WELL AS UP TO 40 YEARS UNDER CONSTANT AMBIENT TEMPERATURE

With the aforementioned determined and calibrated gasket element model, the mechanical seal behaviour depending on temperature and time can be investigated in an entire cask model, see Figure 6 a). Where, the defined gasket element was implemented in the lid system of this cask model, see Figures 6 b) and c), which was prior used for FE analyses regarding accident conditions from an airplane crash with subsequent fires or debris loads, see the work of Droste, B., et al. (2002) and Wieser, G., et al. (2004).

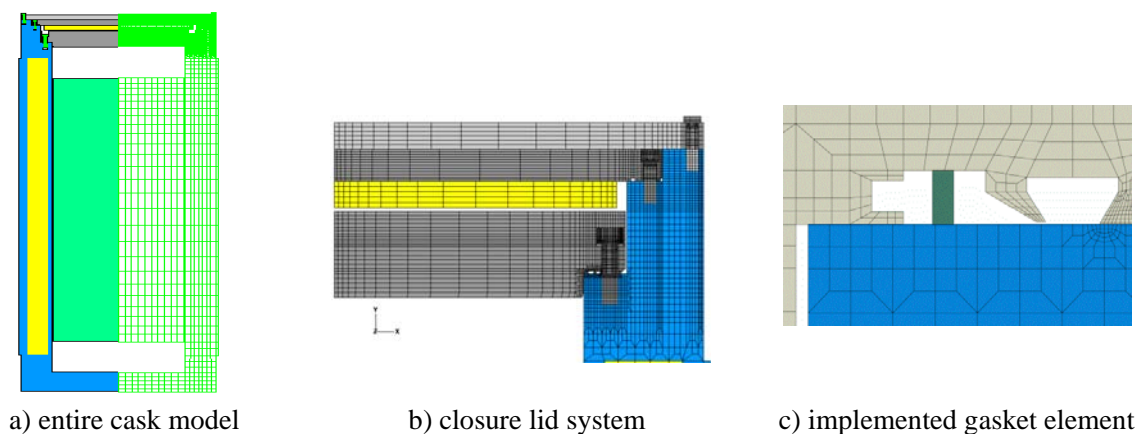


Figure 6. a) FE model of a transport and storage cask and b) detailed lid system with c) assembled gasket element in notch of the primary lid.

Figure 6 a) shows an entire cask model which includes cask body with moderator zone, basket (as inner heat source), primary lid, moderator plate, secondary lid, protective cover plate and bolting of the lid system. A more detailed extract of the lid system is shown in Figure 6 b). The chosen discretization

ensures the necessary exactitude of displacement calculations of seal position with different bolt pre-tension force and different thermal-mechanic loads. The implemented gasket element in notch of the primary lid is shown in Figure 6 c). The contact condition between cask body and lid surface was defined as “small sliding” contact with friction. The width of gasket element was chosen equal to the measured mean contact width of a seal loaded to the specific working point.

The gross weight of those casks is approximately 125 Mg. The complete FE model has about 5000 elements and 5400 nodes. It was built up with 2D axial symmetric solid elements of ABAQUS type DCAX4 with linear interpolation for fire load simulation and CAX4R with linear interpolation and reduced integration for the static and dynamic load simulation. All free surfaces (between cask body and basket, cask body and primary/secondary lid, cask body and protective cover as well as between bolt head and primary/secondary lid) were defined by using ABAQUS option "general contact" with friction. Very complex thermal boundary conditions were given in a prior work, see Wieser, G., et al. (2004).

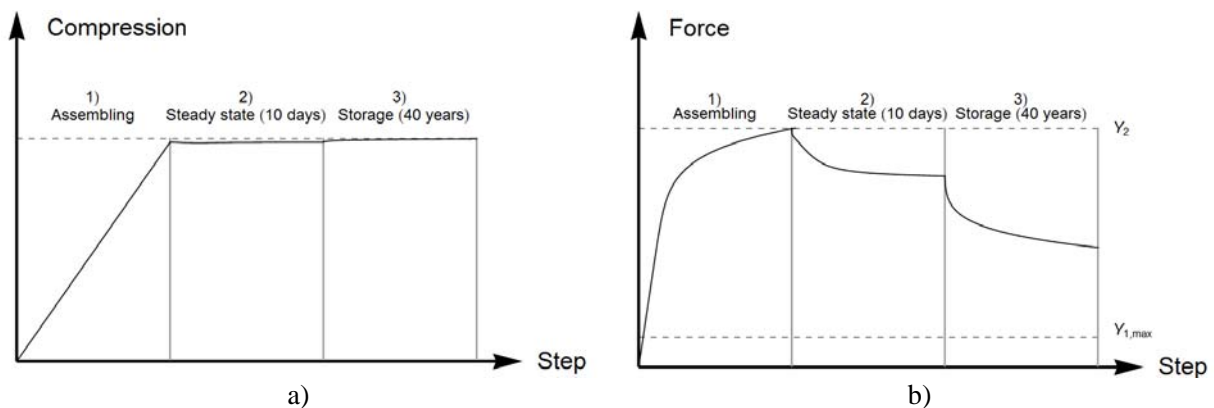


Figure 7. Example of a) seal compression and b) seal force depending on simulation steps with constant ambient temperature and constant released heat.

Three main simulation steps were carried out: 1) initial assembling of lid system, 2) increasing in temperature up to steady-state conditions due to the related heat emission and 3) constant or decreasing in temperature during storage period up to 40 years. These steps are shown in Figure 7 with constant ambient temperature and constant released heat emission. In the first step, the lid-system of the cask was assembled with pre-tension of bolts under ambient temperature. The studied metal gasket of the primary lid was loaded to the specific working point. In a second step, the cask temperature rises to the steady-state condition in approximately 10 to 20 days due to the decay heat of radioactive waste loaded in casks. For the second step, the change of seal force of metal seals should be considered due to the ‘high relaxation-rate’ in short time. In this step, the temperature of seals rises from the assembling temperature to steady-state temperature conditions. Because of thermal-expansion of the entire lid-system, the compression of seal is mildly reduced but insignificant small, see step 2 in Figure 7 a). Due to this very small compression change, the seal force is unloaded along its elastic unloading line with C_0 and at the same time reduced due to ‘relaxation’ with time and temperature, see step 2 in Figure 7 b). Following the steady-state, in a third step the metal seal behavior can be determined during storage conditions up to 40 years considering constant or changed temperature conditions due to constant or changed decay heat.

In step 2, the change of seal temperature with time up to the steady-state is presented in Figure 8 a) with two different states (I means free-standing or isolated cask and II means collective standing casks) without presentation of corresponding absolute value of maximal temperatures due to the fact that those values are very sensible to ambient temperature, special structure of casks, loaded spent nuclear fuel, heat exchanging conditions of cask surface and storage positions in the building. Furthermore, the given paper

aims to describe a conceptual approach. Calculation of temperature distribution of casks and corresponding absolute values of temperature are not the focus of this work. Presented examples are only used to describe “How to calculate the restoring seal force with different seal temperatures of an assembled metal seal in a real cask”. Corresponding seal force relaxation rate from assembling to steady-state conditions is shown in Figure 8 b).

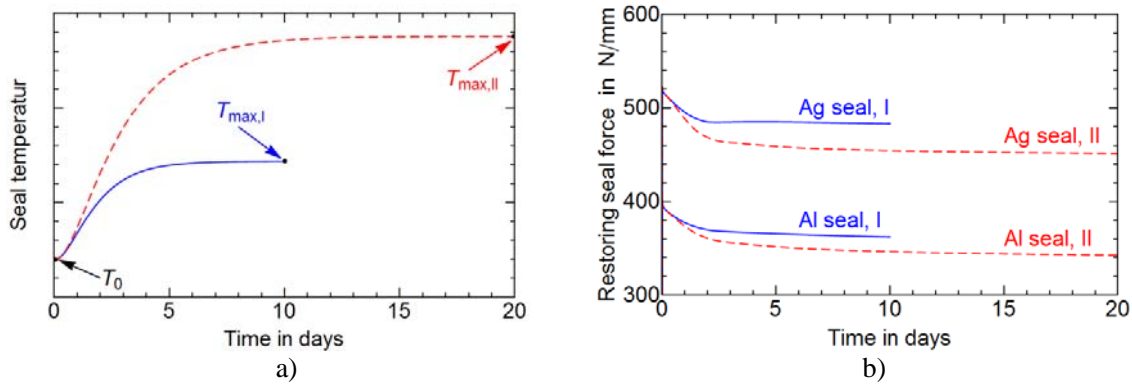


Figure 8. Example of a) seal temperatures and b) restoring seal forces up to steady-state condition under constant ambient temperature but two different states (I and II).

In step 3, long-term creep and relaxation effects of metal seals must be considered during the interim storage period. In principle, the inner heat from spent nuclear fuel shall reduce with time depending on the radioactive inventory. It can be approximately defined with exponential decay law as

$$Q(t) = Q_{\infty} + (Q_0 - Q_{\infty})e^{-\lambda(t/t_0)^{\beta}} . \quad (7)$$

Whereat, Q_0 is the inner heat at the beginning of storage, Q_{∞} is the residual heat, t_0 is used to normalize the time, λ and β are the decay constants of the stored spent fuel material. A typical change of heat emission and its influence of seal temperature are shown in Figure 9.

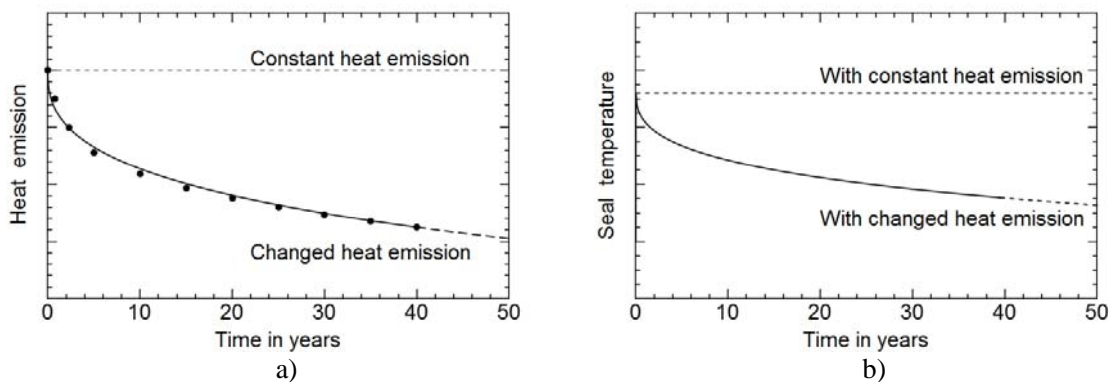


Figure 9. Example of a) heat emission state and b) seal temperature of a stored cask up to 40 years.

The points in Figure 9 a) are values from sophisticated calculations of a spent fuel material. The black line diagrams a fitting curve from Equation 7. If the heat emission is constant, then the seal temperature is constant, too. For changed heat emission, the seal temperature will reduce with time, see Figure 9 b).

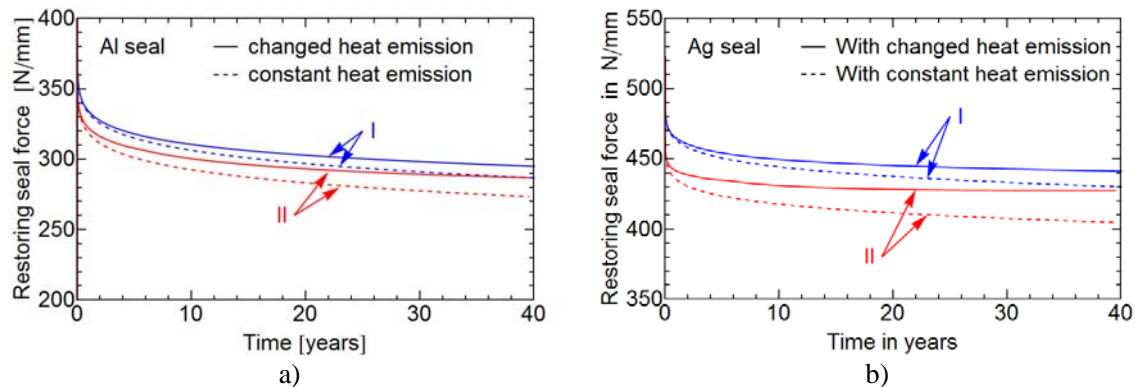


Figure 10. Estimated seal force behaviour of a) Al-seals or b) Ag-seals from FE calculation of a transport and storage cask in time up to 40 years with constant or changed heat emission under constant ambient temperature but two different states (I and II).

Results of relaxation simulations from step 3 with constant and changed heat emission under constant ambient temperature are shown in Figure 10. For the exemplarily chosen typically and realistic inventory as well as boundary conditions, even until 40 years, the restoring seal force is above 50 % of the initial seal force. But, investigations about the same sealing type with constant test temperature of 150 °C show, that the restoring seal force decreases notably less than 50 % of the initial seal force within one year. In principle, the decreasing of seal force is mainly effected by temperature.

CONCLUSIONS

Based upon experimental results, a global gasket element model was calibrated, verified and used for the evaluation of metal seal behaviour of a transport and storage cask under interim storage conditions up to 40 years in a storage facility, in Germany. The global behaviour of metal seals in lid-systems of transport and storage casks under storage conditions was studied using a FE model with a specific gasket element type. Geometrical conditions of a lid system and corresponding thermal expansion, as well as the influence of time and temperature related to metal seals assembled in casks can be estimated. With the knowledge of temperature dependency, the developed calculation model for the seal force behaviour is suitable to evaluate time-temperature dependant restoring seal force values under real storage conditions.

REFERENCES

- ABAQUS (2014), Abaqus User's Guide, Dassault Systèmes.
 Droste, B., Völzke H., Wieser G. and Qiao L. (2002). "Safety Margins of Spent Fuel Transport and Storage Casks Considering Aircraft Crash Impacts", *Packaging, Transport, Storage and Security of Radioactive Material*, RAMTRANSPORT Publishing, Vol. 13, No. 3-4, 313-316.
 Garlock (2001). HELICOFLEX® Catalogue, Reference HEL1, BFGoodrich.
 Ledrappier, F., et al. (2016). "Numerical Simulation of HELICOFLEX® Metallic Gasket Ageing Mechanism for Spent Fuel Cask", *18th Int. Symposium on the Packaging and Transportation of Radioactive Materials (PATRAM 2016)*, Kobe, Japan.

- Nagelschmidt, S., Herbrich, U., Probst, U., Wolff, D. and Völzke, H. (2014). “Test Results and Analyses in Terms of Aging Mechanisms of Metal Seals in Casks for Dry Storage of SNF – 14255”, *Waste Management Conference 2014 (WM2014)*, Phoenix, Arizona, USA.
- Nakamura, K., Takayanagi, T. and Sato S. (1989). “A Modified Arrhenius Equation”, *Chemical Physics Letters*, Vol. 160, No. 3, 295-298.
- Probst, U., Schulz, S., Jaunich, M., Wolff, D. and Völzke, H. (2014). “Langzeituntersuchungen an Metaldichtung für Transport- und Lagerbehälter für radioaktive Stoffe”, *Dichtungstechnik Jahrbuch 2014*, 162-173, ISGATEC GmbH, Mannheim.
- Qiao, L., Zencker, U., Herbrich, U., Nagelschmidt, S. and Völzke, H. (2016). “Modelling Long-term Relaxation of Metal Seals for Transport and Storage Casks”, *2016 EMI International Conference*, Metz, France.
- Qiao, L., Nagelschmidt, S. Herbrich, U., Wolff, D., Zencker, U., and Völzke, H. (2017). “Application of Time-Temperature Superposition Principle with a Modified Arrhenius Equation for the Relaxation Analysis of Metal Seals”, *2017 EMI International Conference*, San Diego, USA.
- Sassoulas, H., et al. (2006). “Ageing of Metallic Gaskets for Spent Fuel Casks: Century-long Life Forecast from 25,000-h-long Experiments”, *Nuclear Engineering and Design*, vol. 236, 2411-2417.
- Shirai, K., et al. (2013). “Numerical Evaluation of the Long-term Sealing Performance of the Silver Gasket for Dual Purpose metal Cask under High Temperature”, *17th Int. Symposium on the Packaging and Transportation of Radioactive Materials (PATRAM 2013)*, San Francisco, CA USA.
- Völzke, H., Wolff, D., Probst, U., Nagelschmidt, S. and Schulz S. (2013). “Long-term Performance of Metal Seals for Transport and Storage Casks”, *17th Int. Symposium on the Packaging and Transportation of Radioactive Materials (PATRAM 2013)*, San Francisco, CA USA.
- Wieser, G., Qiao, L., Völzke, H., Wolff, D. and Droste, B. (2004). “Safety Analysis of Gasket under Extreme Impact Conditions”, *Packaging, Transport, Storage and Security of Radioactive Material*, RAMTRANSPORT Publishing Vol. 15, No.2, 141-147.
- Wieser, G., Qiao, L., Eberle, A. and Völzke, H. (2004). “Thermo-Mechanical Finite Element Analyses of Bolted Cask Lid Structures”, *Packaging, Transport, Storage and Security of Radioactive Material*, RAMTRANSPORT Publishing, Vol. 15, Nos.3-4, 223-230.
- Zencker, U., Qiao, L. and Völzke, H. (2015). “Strategies for Numerical Modelling of Metal Gaskets in Transport and Storage Casks”, *Radioactive Materials Transport and Storage Conference and Exhibition (RAMTRANSPORT 2015)*, Oxford, United Kingdom.